

Wavepacket dynamics in energy space, RMT and quantum-classical correspondence

Doron Cohen¹, Felix M. Izrailev² and Tsampikos Kottos³

¹ Department of Physics, Harvard University, Cambridge, MA 02138

² Instituto de Fisica, Universidad Autonoma de Puebla, Puebla, Pue 72570, Mexico

³ Max-Planck-Institut für Strömungsforschung, 37073 Göttingen, Germany

(November 1999, to be published in Phys. Rev. Lett.)

We apply random-matrix-theory (RMT) to the analysis of evolution of wavepackets in energy space. We study the crossover from ballistic behavior to saturation, the possibility of having an intermediate diffusive behavior, and the feasibility of strong localization effect. Both theoretical considerations and numerical results are presented. Using quantal-classical correspondence (QCC) considerations we question the validity of the emerging dynamical picture. In particular we claim that the appearance of the intermediate diffusive behavior is possibly an artifact of the RMT strategy.

We are interested in the dynamics that is generated by a Hamiltonian of the type $\mathcal{H} = \mathbf{E} + \mathbf{W}$ where \mathbf{E} is a diagonal matrix whose elements are the ordered energies $\{E_n\}$, with mean level spacing Δ , and \mathbf{W} is a banded matrix. It is assumed that \mathbf{W} is similar to a ‘Banded Random Matrix’ (BRM), with non-vanishing couplings within the band $0 < |n - m| \leq b$. These coupling elements are zero on the average, and they are characterized by the variance $\sigma = (|\mathbf{W}_{nm}|^2)^{1/2}$. Thus, there are four parameters $(\Delta, b, \sigma, \hbar)$ that controls the dynamics. One important application of BRM is in solid-state physics for the study of localization in quasi-one-dimensional disordered systems. In this frame non-zero values of Δ reflect the presence of a constant electric field along the sample. However, in this Letter we mainly have in mind the original motivation following Wigner [1]. Namely, the study of either *chaotic* or complex conservative quantum systems that are encountered in nuclear physics as well as in atomic and molecular physics. For this reason the above defined model (with non-zero Δ) is known in the literature [2–4] as Wigner’s BRM (WBRM) model.

Consider a system whose total Hamiltonian is $\mathcal{H}(Q, P)$, where (Q, P) is a set of canonical coordinates. We assume that the preparation and the representation of the system are determined by a Hamiltonian $\mathcal{H}_0(Q, P)$. We also assume that both $\mathcal{H}_0(Q, P)$ and $\mathcal{H}(Q, P)$ generate classically chaotic dynamics of similar nature¹. We choose a basis such that the quantized Hamiltonian matrix \mathcal{H}_0 has a diagonal structure $\mathcal{H}_0 = \mathbf{E}$. According to general semiclassical arguments [2], the quantized Hamiltonian matrix \mathcal{H} , in the same basis, has a band structure $\mathcal{H} = \mathbf{E} + \mathbf{W}$. The WBRM model can be regarded as a *simplified* local description of the true Hamiltonian matrix. However, there is one feature that distinguishes the effective WBRM model from the true Hamiltonian. It is the assumption that the off-diagonal elements are *uncorrelated*, as if they were independent random numbers. In this Letter we would like to explore the consequences of this RMT assumption on the dynamics. Below we define the classical limit of the WBRM-model, and the various parametric regimes in the quantum-mechanical theory. We analyze the dynamical scenario in each regime, and we explain that the emerging picture is incompatible with the quantal-classical correspondence (QCC) principle.

Taking $\mathcal{H}(Q, P)$ to be a generator for the (classical) dynamics, the energy $\mathcal{H}_0(t) = \mathcal{H}_0(Q(t), P(t))$ fluctuates. The fluctuations are characterized by a correlation time τ_{cl} , and by an amplitude δE_{cl} . The three parameters (Δ, b, σ) that define the effective WBRM model are determined by semiclassical considerations [2]. One obtains $\Delta \propto \hbar^d$, and $b \propto \hbar^{-(d-1)}$, and $\sigma \propto \hbar^{(d-1)/2}$, where d is the number of degrees of freedom (dimensionality) of the system. In this Letter, we find it convenient to *define*² the two classical quantities $(\tau_{cl}, \delta E_{cl})$ in terms of the common quantum-mechanical parameters:

$$\tau_{cl} = \hbar/(b\Delta) \quad , \quad \delta E_{cl} = 2\sqrt{b} \sigma \quad (1)$$

The classical dynamical scenario is formulated by using a phase-space picture [5]. The initial preparation is assumed to be a microcanonical distribution that is supported by one of the energy-surfaces of $\mathcal{H}_0(Q, P)$. For $t > 0$, the phase-space distribution spreads away from the initial surface. ‘Points’ of the evolving distribution move upon the energy-surfaces of $\mathcal{H}(Q, P)$. We are interested in the distribution of the energies $\mathcal{H}_0(t)$ of the evolving ‘points’. It is easily argued that for short times this distribution evolves in a ballistic fashion. Then, for $t \gg \tau_{cl}$, due to ergodicity, a ‘steady-state distribution’ appears, where the evolving ‘points’ occupies an ‘energy shell’ in phase-space. The thickness of this energy shell [4] equals δE_{cl} . Thus we have a crossover from ballistic energy spreading to saturation. The dynamics in the classical limit is fully characterized by the two classical parameters τ_{cl} and δE_{cl} .

We are going to study the corresponding quantum-mechanical scenario. We want to explore the consequences of assuming that WBRM model can be used as an effective model for the true dynamics. At $t = 0$ the system is prepared in an eigenstate of $\mathcal{H}_0 = \mathbf{E}$. For $t > 0$ the evolution of the system is determined by $\mathcal{H} = \mathbf{E} + \mathbf{W}$. The evolving state is $\psi(t)$, and we are interested in the evolving distribution $|\langle n | \psi(t) \rangle|^2$. We shall use the following terminology: The standard perturbative regime is $(\sigma/\Delta) \ll 1$; The Wigner regime is $1 \ll (\sigma/\Delta) \ll b^{1/2}$; The ergodic regime is $b^{1/2} \ll (\sigma/\Delta) \ll b^{3/2}$; The localization regime is $b^{3/2} \ll (\sigma/\Delta)$. See [1,4]. It is easily verified that the limit $\hbar \rightarrow 0$ corresponds to the ergodic regime or possibly (provided $d = 2$) to the localization regime.

The structure of the eigenstates α of \mathcal{H} has been studied in [1,3,4]. We denote the average shape of an eigenstate as $W_E(r) = \langle |\varphi_\alpha(n_\alpha + r)|^2 \rangle$ where $\varphi_\alpha(n) = \langle n|\alpha \rangle$, and n_α is the 'site' around which the eigenstate is located. The average is taken over all the eigenstates that have roughly the same energy $E_\alpha \sim E$. There are two important energy scales: One is the classical width of the energy shell δE_{cl} , and the other is the range of the interaction $\Delta_b = b\Delta$. In the *standard perturbative regime* $W_E(r)$ contains mainly one level, and there are perturbative tails that extend over the range Δ_b . In the *Wigner regime*, many levels are mixed: the main (non-perturbative) component of $W_E(r)$ has width $\Gamma = 2\pi(\sigma/\Delta)^2 \times \Delta$, and the shape within the bandwidth Δ_b is of Lorentzian type. However in actual physical applications this Lorentzian is a special case of core-tail structure [5], where the tail can be found via first order perturbation theory. Outside the bandwidth the tails decay faster than exponentially [3]. On approach to the ergodic regime $W_E(r)$ spills over the range Δ_b . Deep in the *ergodic regime* it occupies 'ergodically' the whole energy shell whose width is δE_{cl} . In actual physical applications the exact shape is determined by simple classical considerations [5,6]. Deep in the *localization regime* $W_E(r)$ is no longer ergodic: A typical eigenstate is exponentially localized within an energy range $\delta E_\xi = \xi\Delta$ much smaller than δE_{cl} . The localization length is $\xi \approx b^2$. In actual physical applications it is not clear whether there is such type of localization. To avoid confusion, we are going to use the term 'localization' only in the sense of having $\delta E_\xi \ll \delta E_{cl}$.

Now we would like to explore the various dynamical scenarios that can be generated by the Schrödinger equation for $a_n(t) = \langle n|\psi(t) \rangle$. Namely,

$$\frac{da_n}{dt} = -\frac{i}{\hbar} E_n a_n - \frac{i}{\hbar} \sum_m \mathbf{W}_{nm} a_m \quad (2)$$

starting with an initial preparation $a_n = \delta_{nm}$ at $t=0$. In a previous study [7] only the localization regime has been considered. Here we are going to consider the general case ($\Delta \neq 0$). We describe the energy spreading profile for $t > 0$ by the transition probability kernel $P_t(n|m) = \langle |a_n(t)|^2 \rangle$. The angular brackets stand for averaging over realizations of the Hamiltonian. In particular, it is convenient to characterize the energy spreading profile by the variance $M(t) = \sum_n (n-m)^2 P_t(n|m)$, and by the participation ratio $N(t) = (\sum_n (P_t(n|m))^2)^{-1}$, and by the total transition probability $p(t)$, and by the out-of-band transition probability $q(t)$. Both $p(t)$ and $q(t)$ are defined as $\sum'_n P(n|m)$ where the prime indicate exclusions of the term $n = m$ or exclusion of the terms $|n-m| \leq b$ respectively. Equation (2) has been integrated numerically using the self-expanding algorithm of [7] to eliminate finite-size effects. Namely, additional $10b$ sites are added to each edge whenever the probability of finding the 'particle' at the edge sites exceeded 10^{-15} . Fig.1 illustrates the time-evolution of the energy spreading profile. From such plots we can define

various time scales. The times t_{ball} and t_{sat} pertains to $M(t)$ and mark the departure-time from ballistic behavior and the crossover-time to saturation. The time t_{sta} pertains to $N(t)$ and marks the crossover to a stationary distribution. The time scale t_{prt} pertains to $p(t)$ and marks the disappearance of the simple perturbative structure (See (3) below). The asymptotic value of $q(t)$, if it is much less than 1, indicates that the system is either in the standard perturbative regime or in the Wigner regime, where out-of-band transitions can be neglected. The saturation profile is given by the expression $P_\infty(n|m) = \sum_\alpha |\langle n|\alpha \rangle|^2 |\langle \alpha|m \rangle|^2$, and it is roughly approximated by the auto-convolution of $W_E(r)$. Therefore the saturation profiles (Fig.1) are similar to the average shape of the eigenstates. We have found that $M(\infty)$ satisfies a scaling relation $Y = 2X \cdot (1 - \exp(-1/(2X)))$ where $X = (\sigma/\Delta)/b^{3/2}$ and $Y = (M(\infty))^{1/2}/b^2$. This scaling relation is similar to the one that pertains to the average shape of the eigenstates [4].

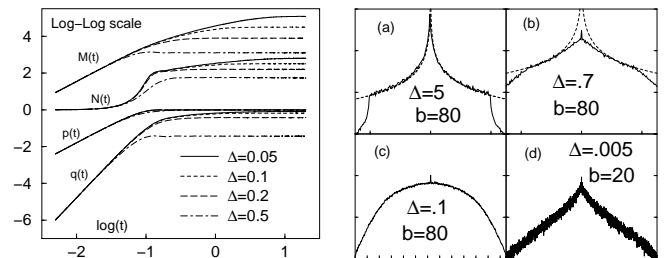


FIG. 1. *Left figure:* Representative examples for the time-evolution of the energy spreading profile. The variance $M(t)$, the participation ratio $N(t)$, the total transition probability $p(t)$, and the out-of-band transition probability $q(t)$ are plotted for $\Delta=0.05, 0.10, 0.20, 0.50$ and $b=80$. The units of energy are chosen such that $\sigma=1$ and the units of time such that $\hbar=1$. *Right figures:* Saturation profiles for various regimes: (a) Standard perturbative regime; (b) Wigner regime; (c) Ergodic regime; (d) Localization regime. The distance between the tick-marks on the horizontal axis of (a)-(c) is b . In (d) the full scale is $|n-m| < 2000$. The full scale of the vertical log-axis is $-15 < \ln(P) < 0$. Note that the $n=m$ term is factor 3 larger compared with its immediate vicinity [7]. In (a) and (b) the $1/(n-m)^2$ behavior of the (in-band) tail is fitted by dashed lines. Notice the appearance of a core region in (b), indicated by the 'flattening' of the profile for $|n-m| < 20$. The in-band profile in (b) corresponds to a Lorentzian with a very high accuracy.

In the *standard perturbative regime* each eigenstate of \mathcal{H} is localized 'perturbatively' in one energy level. Thus, for arbitrarily long times the probability is concentrated mainly in the initial level. We can write schematically [5]

$$P_t(n|m) \approx \delta_{nm} + \text{Tail}(n-m; t) \quad (3)$$

where $\text{Tail}(n-m; t) = (\sigma/\hbar)^2 t \tilde{F}_t((E_n - E_m)/\hbar)$ within the range of first order transitions ($0 < |n-m| < b$), and zero otherwise. Here $\tilde{F}_t(\omega) = t \cdot (\text{sinc}(\omega t/2))^2$ is the spectral-content of a constant perturbation of duration t , and $\text{sinc}(x) = \sin(x)/x$. We have trivial recurrences from n to m once t becomes larger than $2\pi\hbar/(E_n - E_m)$. The

global crossover to quasi-periodic behavior is marked by the Heisenberg time $t_H = 2\pi\hbar/\Delta$. The total normalization of the tail is much less than unity at any time.

In the *Wigner regime*, one observes that the perturbative expression (3) is still valid for sufficiently short times $t \ll t_{\text{prt}}$. Let us estimate the perturbative break-time t_{prt} . For short times ($t < \tau_{\text{cl}}$) the spectral function $\tilde{F}_t(\omega)$ is very wide compared with the bandwidth Δ_b of first-order transitions. Consequently we can use the replacement $\tilde{F}_t(\omega) \mapsto t$ and we get that the total transition probability is $p(t) \approx b \times (\sigma t/\hbar)^2$. On the other hand, for $t > \tau_{\text{cl}}$, the spectral function $\tilde{F}_t(\omega)$ is narrow compared with the bandwidth, and it can be approximated by a delta-function. As a result we get $p(t) \approx \sigma^2/(\hbar\Delta) \times t$. The condition $p(t) \sim 1$ determines t_{prt} leading to:

$$t_{\text{prt}} = \begin{cases} \hbar\Delta/\sigma^2 & \text{for } 1 < \sigma/\Delta < \sqrt{b} \\ \hbar/(\sqrt{b}\sigma) & \text{for } \sqrt{b} < \sigma/\Delta \end{cases} \quad (4)$$

It should be noticed that for $\sigma \sim \Delta$ we get $t_{\text{prt}} \sim t_H$. Thus, taking recurrences into account, we come again to the conclusion, that for $\sigma \ll \Delta$ there is no perturbative breaktime. The *variance* $(\delta E(t))^2 = \Delta^2 \times M(t)$ of the energy distribution (3) is easily calculated. We get a ballistic-like behavior, followed by saturation,

$$\delta E(t) \approx \begin{cases} (\delta E_{\text{cl}}/\tau_{\text{cl}}) t & \text{for } t < \tau_{\text{cl}} \\ \delta E_{\text{cl}} & \text{for } t > \tau_{\text{cl}} \end{cases} \quad (5)$$

For $t \sim t_{\text{prt}}$ the tail (3) becomes Lorentzian-like, and it is characterized by a width $\hbar/t = \Gamma$. For $t > t_{\text{prt}}$ expression (3) loses its validity, but it is obvious that the energy cannot spread any more, since it had already acquired the saturation profile.

It should be realized that neither (3), nor the Lorentzian-like saturation profile of the Wigner regime, could correspond to the classical spreading profile. In the latter case the saturation profile is characterized by two genuine quantum mechanical scales (Γ, Δ_b), whereas the classical ergodic distribution is characterized by the single energy scale δE_{cl} . See Fig.2. However, in spite of this lack of correspondence, the variance (5) behaves in a classical-like fashion. Using the terminology of [5] we have here *restricted* rather than *detailed* quantal-classical correspondence (QCC): The quantal $P_t(n|m)$ is definitely different from its classical analog, but the variance $\delta E(t)$, unlike the higher moments of the distribution, turns out to be the same.

In the *ergodic regime* the time scale τ_{cl} becomes larger than t_{prt} , and therefore τ_{cl} loses its significance. At $t \sim t_{\text{prt}}$ the quantal energy-spreading just "fills" the energy range Δ_b , and we get $\delta E(t) \approx \Delta_b$. The perturbative result (3) is no longer applicable for $t > t_{\text{prt}}$. However, the simplest heuristic picture turns out to be correct. Namely, once the mechanism for ballistic-like spreading disappears a stochastic-like behavior takes its place. The stochastic energy spreading is similar to a random-walk process where the step size is of the order Δ_b , with transient time equals t_{prt} . Therefore we have a diffusive behavior $\delta E(t)^2 = D_E t$ where

$$D_E = C \cdot \Delta_b^2/t_{\text{prt}} = C \cdot \Delta^2 b^{5/2} \sigma/\hbar \propto \hbar \quad (6)$$

and the numerical prefactor [7] is $C \approx 0.85$. This diffusion is not of classical nature. The diffusion can go on as long as $(D_E t)^{1/2} < \delta E_{\text{cl}}$, hence the ergodic time is

$$t_{\text{erg}} = b^{-3/2} \hbar \sigma/\Delta^2 \propto 1/\hbar \quad (7)$$

After this ergodic time the energy spreading profile saturates to a classical-like steady state distribution [4].

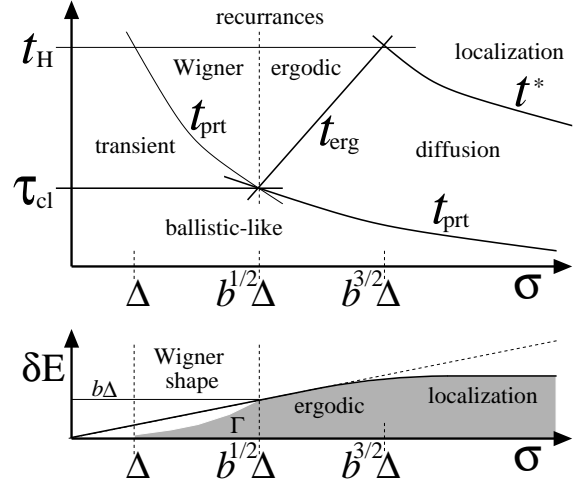


FIG. 2. The *upper diagram* illustrates the various dynamical scenarios which are described in the text. The flow of time is in the vertical direction. See [8] for closely related diagrams. The *lower plot* illustrates the various energy-scales that characterize the associated stationary distributions: The bandwidth Δ_b is indicated by a horizontal solid line; The width of the non-perturbative component is indicated by the grey filling; The width of the energy shell is indicated by the dashed line; The variance $\delta E(\infty)$ is indicated by the bold solid line. In the localization regime we have $\delta E(\infty) \approx \delta E_\xi \ll \delta E_{\text{cl}}$.

In the *localization regime* the quasi periodic nature of the dynamics is important. The ‘operative’ eigenstates are defined as those having a non-negligible overlap with the initial state m . These eigenstates are located within the energy shell whose width is δE_{cl} . If the eigenstates are ergodic, then all of them are ‘operative’, and therefore the effective level spacing between them is simply $\Delta_{\text{eff}} \approx \Delta$. However, if the eigenstates are localized, then only ξ out of them have a significant overlap with the initial state m , and therefore the effective level spacing is $\Delta_{\text{eff}} \approx \delta E_{\text{cl}}/\xi$. The effective energy spacing Δ_{eff} is the relevant energy scale for determination of the crossover to quasiperiodic behavior. The associated time scale is $t^* = 2\pi\hbar/\Delta_{\text{eff}}$, and it may be either less than or equal to the Heisenberg time $t_H = 2\pi\hbar/\Delta$. The localization regime is defined by the condition $t^* < t_{\text{erg}}$. In this regime the diffusion stops before an ergodic distribution arises, and we should get $D_E t^* \approx \delta E_\xi^2$. Inserting the definition of t^* and solving for ξ we obtain the well known [2,4] estimate $\xi \approx b^2$. For the breaktime we obtain

$$t^* = b^{3/2} \hbar / \sigma \propto (1/\hbar)^{2d-3} \quad (8)$$

Note that the localization range is $\delta E_\xi = \xi \Delta \propto (1/\hbar)^{d-2}$. If the diffusion were of classical nature, we would get $\delta E_\xi \propto (1/\hbar)^{d-1}$ as in the semiclassical analysis of [8].

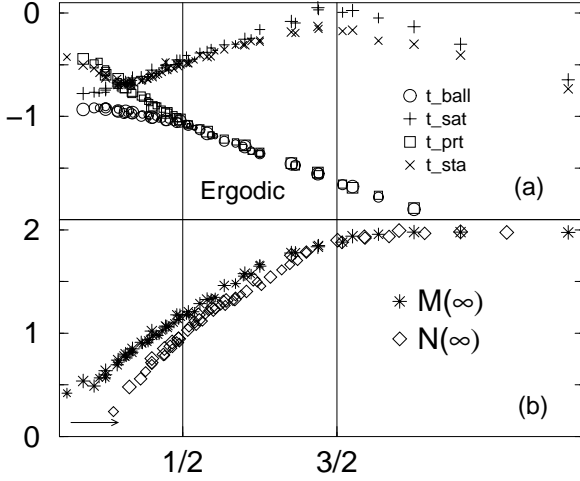


FIG. 3. (a) The times t_{ball} , t_{sat} , t_{sta} and t_{prt} are numerically determined. Different values of b are distinguished by the relative size of the symbols. The axes are $X = \log(\sigma/\Delta)/\log(b)$, and $Y = \log(t/t_H)/\log(2\pi b)$. Note that $Y = -1$ implies $t = \tau_{\text{cl}}$, and $Y = 0$ implies $t = t_H$. In the ergodic regime t_{sat} departs from t_{bal} and an intermediate diffusive stage appears. The saturation time approaches t_H but eventually drops down once we enter into the localization regime. (b) Both $\log(M(\infty))/\log(b)$ and $\log(N(\infty))/\log(b)$ are plotted versus $\log(\sigma/\Delta)/\log(b)$. The arrow indicates a global horizontal shift of the $N(\infty)$ plot for presentation purpose.

The various dynamical scenarios discussed above are summarized by the diagram of Fig.2, and can be compared with the data presented in Fig.3. As expected from the theoretical considerations we have in the Wigner regime $t_{\text{ball}} \approx t_{\text{sat}} \approx \tau_{\text{cl}}$ and $t_{\text{sta}} \approx t_{\text{prt}}$. In the ergodic regime we have as expected $t_{\text{ball}} \approx t_{\text{prt}} \ll \tau_{\text{cl}}$, while $t_{\text{sat}} \approx t_{\text{sta}} \equiv t_{\text{erg}}$. Thus, in the ergodic regime we have a premature departure of the ballistic behavior, and the appearance of an intermediate diffusive stage.

Our major motivation for studying WBRM model comes from ‘quantum chaos’ (see introduction). Namely, WBRM model can be regarded as an effective model for the analysis of the dynamics of a ‘quantized’ classically chaotic system. The condition to be in the regime $(\sigma/\Delta) \ll b^{1/2}$ can be cast into the form $\hbar \gg C_{\text{prt}}$, where $C_{\text{prt}} = \delta E_{\text{cl}} \tau_{\text{cl}}$ is a classical scale. In this regime the *perturbative* result Eq.(5) is valid. The derivation of (5) is not sensitive to the presence or the absence of subtle correlations between matrix elements. Therefore (5) is valid in case of the ‘quantized’ Hamiltonian, as well as in case of the effective WBRM model. Hence we may say that the applicability of an effective RMT approach is *trivial* in the regime $\hbar \gg C_{\text{prt}}$. In contrast to that, in the *non-perturbative* regime ($\hbar \ll C_{\text{prt}}$), correlations between matrix elements become important, and it may have implications on the dynamical behavior. Whether

an effective RMT approach is valid becomes a *non-trivial* question in the non-perturbative regime.

In the regime $\hbar \gg C_{\text{prt}}$ we have restricted QCC [5]. It means that QCC holds *only* for the variance $\delta E(t)$. Fixing all the classical parameters, including the time t which is assumed to be of the order of τ_{cl} , we can always define a sufficient condition $\hbar \ll C_{\text{SC}}$ for having detailed QCC [5]. Detailed QCC means that the quantal energy spreading profile $P_t(n|m)$ can be approximated by a classical calculation. The considerations that lead to the determination of the classical scale C_{SC} are discussed in [5]. We cannot give an explicit expression for C_{SC} because it is a non-universal (system-specific) parameter. Detailed QCC implies that Eq.(5) should hold again once the condition $\hbar \ll C_{\text{SC}}$ is satisfied.

For the WBRM model we have found that for $\hbar \ll C_{\text{prt}}$ there is a pre-mature departure from ballistic behavior, followed by an intermediate diffusive behavior. So we have a contradiction here between RMT considerations on one hand, and QCC considerations on the other. Thus, if the RMT approach is non-trivially valid, then it is only in a restricted range $C_{\text{SC}} \ll \hbar \ll C_{\text{prt}}$. Outside this regime it is either trivially valid ($\hbar \gg C_{\text{prt}}$) and we have restricted QCC, or else it is not valid at all ($\hbar \ll C_{\text{SC}}$) and instead we have detailed QCC. It may be true that in many cases the RMT considerations are not valid for the purpose of analyzing time-dependent dynamical scenarios. A similar situation may arise in the theory of quantum dissipation: There is one-to-one correspondence between the regimes in Fig.5 of [5] and the regimes that have been discussed in this Letter.

We thank the MPI für Komplexer Systeme in Dresden for the kind hospitality during the Conference *Dynamics of Complex Systems* where this work was initiated. F.M.I acknowledges support by CONACyT (Mexico) Grants No. 26163-E and 28626-E.

[†] Physically, going from \mathcal{H}_0 to \mathcal{H} may signify a change of an external field, or switching on a perturbation, or sudden change of effective-interaction (as in molecular dynamics).

[‡] The numerical prefactors are chosen such that whenever (5) applies, we have $t_{\text{bal}} = \tau_{\text{cl}}$ and $\delta E(\infty) = \delta E_{\text{cl}}$.

- [1] E. Wigner, Ann. Math **62** 548 (1955); **65** 203 (1957).
- [2] M. Feingold and A. Peres, Phys. Rev. A **34** 591, (1986).
- [3] M. Feingold, D. Leitner, M. Wilkinson, Phys. Rev. Lett. **66**, 986 (1991); M. Feingold et al., PRL **70**, 2936 (1993).
- [4] V.V. Flambaum, A.A. Gribakina, G.F. Gribakin and M.G. Kozlov, Phys. Rev. A **50** 267 (1994).
- [5] G. Casati, B.V. Chirikov, I. Guarneri, F.M. Izrailev, Phys. Rev. E **48**, R1613 (1993); Phys. Lett. A **223**, 430 (1996).
- [6] D. Cohen, Phys. Rev. Lett. **82**, 4951 (1999); cond-mat/9902168. D. Cohen and E. Heller, chao-dyn/9909014.
- [7] F. Borgonovi, I. Guarneri and F.M. Izrailev, Phys. Rev. E **57**, 5291 (1998).
- [8] F.M. Izrailev, T. Kottos, A. Politi, S. Ruffo, G.P. Tsironis, Europhys. Lett. **34**, 441 (1996). F.M. Izrailev, T. Kottos, A. Politi, G.P. Tsironis, Phys. Rev. E **55**, 4951 (1997). A. Politi, S. Ruffo, L. Tessieri, Phys. Rev. E **57**, 5291 (1999).
- [9] D. Cohen, J. Phys. A **31**, 277 (1998).